JOURNAL OF APPLIED ELECTROCHEMISTRY 25 (1995) 187–202

REVIEWS OF APPLIED ELECTROCHEMISTRY 39

Use of electrochemical impedance spectroscopy for the study of corrosion protection by polymer coatings

F. MANSFELD

Corrosion and Environmental Effects Laboratory (CEEL), Department of Materials Science and Engineering, University of Southern California, Los Angeles, CA 90089-0241, USA

Received 25 January 1994; revised 21 June 1994

A discussion of the requirements for hardware and software necessary for collection and analysis of electrochemical impedance spectroscopy data for polymer coated metals is presented. Most authors agree that a simple model can describe the frequency dependence of impedance spectra for polymer coated metals exposed to corrosive environments. The water uptake of the coating can be estimated from the time dependence of the coating capacitance C_c. The pore resistance R_{po} depends both on the resistivity ρ of the coating and the disbonded area A_d. The polarization resistance R_p of the corroding area under the coating and the corresponding capacitance C_{dl} both depend on A_d. The breakpoint frequency method is discussed in detail and the dependence of the breakpoint frequency f_b on ρ and A_d is derived. In addition to f_b other parameters can be obtained which depend on the ratio A_d/ρ or only on A_d or ρ. Since these parameters can be obtained at frequencies exceeding 1 Hz without the need for an analysis of the impedance spectra in the entire frequency region, this approach is considered especially useful for corrosion monitoring. The concepts proposed for the analysis and interpretation of EIS data for polymer coated metals are illustrated using data for Al alloys, Mg and steel exposed to NaCl. For an alkyd coating on cold rolled steel the time dependence of A_d and ρ during exposure to 0.5 M NaCl has been determined qualitatively using the modified breakpoint frequency method.

1. Introduction

One of the most successful applications of electrochemical impedance spectroscopy (EIS) has been in the evaluation of the properties of polymer coated metals and their changes during exposure to corrosive environments. Although it has not been possible in the past to obtain meaningful mechanistic information with traditional d.c. techniques, EIS is now being used in the evaluation of an ever increasing variety of polymer coatings on metals and alloys. Some of the earliest applications of EIS have been devoted to studies of polymer coatings on metals. In this respect, the work of Menges and Schneider [1], who clearly recognized the advantages of the EIS technique, deserves to be mentioned. The impedance modulus was plotted against the frequency of the applied signal in Bode plots as a function of exposure time to 15% HNO_3 at two temperatures for relatively thick (130–260 μm) polyurethane and phenol-formaldehyde coatings on steel. The general model discussed below (Fig. 1(a)) seems to apply and the degradation of the coatings can be clearly followed by changes in the impedance spectra. This series of three papers, which was published in 1973, has unfortunately been cited rarely in the literature. Early applications of EIS in the study of corrosion protection by polymer coatings have been reported by Potente and Braches [2], Scantlebury *et al.* [3], Beaunier *et al.* [4] and by Reinhard *et al.* [5–11] in a seven-part series of papers, which was published in the late 1970s and early 1980s. Beaunier *et al.* [4] used the equivalent circuit in Fig. 1(a), which since then has been applied by the majority of investigators for the analysis of experimental EIS data for polymer coated metals.

The ever increasing literature makes it clear that EIS is ideally suited for the study of polymer coated metals. However, it also is evident that successful application of EIS requires careful design of the experimental approach and use of appropriate hardware for the collection of EIS data as well as suitable software for analysis of experimental data. Since such software is now commercially available, rapid progress has been made in the collection of reliable impedance data and their analysis. Mansfeld and coworkers have developed the Coatfit software for simulation and analysis of EIS data for polymer coated metals [12]. Boukamp's software [13] has been used frequently.

2. Models for the simulation and analysis of EIS data for polymer coated metals and alloys

Most impedance data reported in the literature for polymer coated metals exposed to corrosive media agree with the simple model shown in Fig. 1(a)

0021-891X © 1995 Chapman & Hall

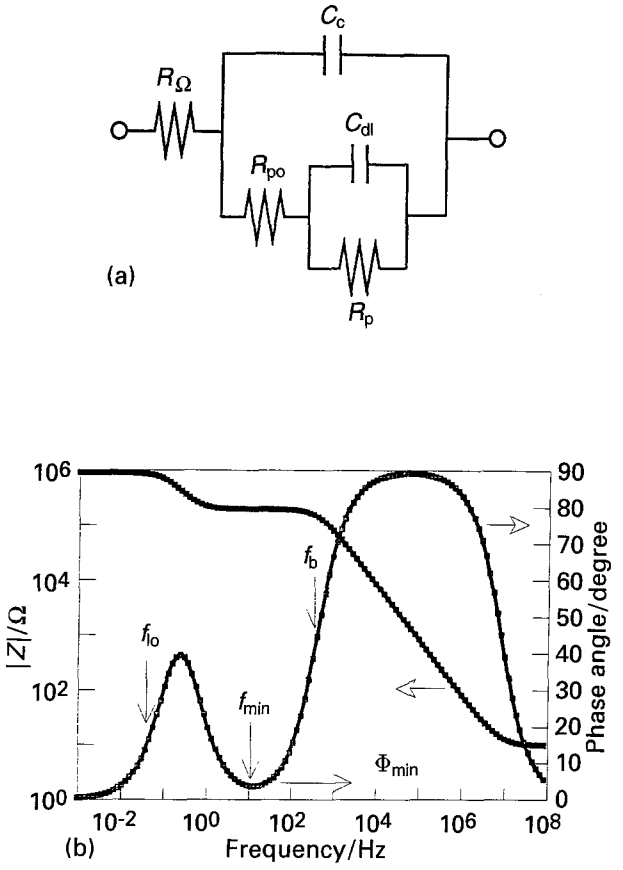

Fig. 1. Model for the impedance of a polymer coated metal (a) and theoretical impedance spectra for a degraded polymer coating (b).

[14–17]. Figure 1(b) shows theoretical Bode plots for a degraded polymer coating according to Fig. 1(a). Certain experimental parameters which have been found useful for the evaluation of coating damage and the extent of corrosion at the metal/coating interface (see below) are indicated in Fig. 1(b). R_Ω corresponds to the uncompensated resistance between reference electrode and test electrode and C_c is the capacitance of the polymer coating given by

$$C_c = \epsilon\epsilon_0 A/d \tag{1}$$

where ϵ is the dielectric constant of the polymer, $\epsilon_0 = 8.85 \times 10^{-14}\,\mathrm{F\,cm^{-1}}$ is the dielectric constant of free space, A is the exposed area of the test electrode and d is the thickness of the coating. For a coating with $d = 35\,\mu\mathrm{m}$ and $\epsilon = 4$ the initial value of C_c is about 100 pF for $A = 1\,\mathrm{cm}^2$. The increase of C_c with exposure time can be used to determine the water uptake of the coating, as will be discussed below. R_{po} is the 'pore resistance' resulting from the formation of ionically conducting paths across the coating [14–17]. R_p is the polarization resistance of the area at the metal/coating interface at which corrosion occurs and C_{dl} is the corresponding capacitance. Since R_{po}, R_p and C_{dl} are related to the delaminated area (also called disbonded or wetted area) A_d:

$$R_{po} = R^o_{po}/A_d = \rho d/A_d \tag{2}$$

$$R_p = R^o_p/A_d \tag{3}$$

$$C_{dl} = C^o_{dl}A_d \tag{4}$$

an estimate of A_d can be obtained from these parameters. It will be noted that R_{po} can decrease due to a decrease of the coating resistance ρ and/or an increase of A_d (Equation 2). Titz *et al.* [18, 19] have estimated the disbonded area based on $C^o_{dl} = 25\,\mu\mathrm{F\,cm^{-2}}$. Armstrong *et al.* [20, 21] have determined C^o_{dl}, R^o_{po} and R^o_p for bare steel and tin and concluded that 'the coatings contain few pores and defects, but when the electrolyte penetrates these and reaches the metal/coating interface rapid delamination of the film occurs'. It is not entirely clear, however, whether data obtained in bulk solutions for bare metals are in agreement with corresponding data for the metal/coating interface for $A_d \to 0$. Kendig *et al.* [22] have commented recently on the relationship between R_{po} and the degree of disbonding of the coating. In their view 'the impedance of an organic coating on a steel surface seems to depend primarily on the transport of ionic species across the coating'.

Occasionally it has been suggested that other impedance elements are added to the equivalent circuit (EC) in Fig. 1(a). Haruyama *et al.* [23] have added a Warburg impedance in series with R_p. However, experimental data which support this assumption are lacking. More recently, Hirayama and Haruyama [24] have proposed a more complicated EC containing three different time constants in order to add the effects of pores in the coating to contributions from the delaminated area previously considered [23]. However, the experimental data reported by Hirayama and Haruyama [24] and by the majority of other workers do not support such a complicated EC. Mansfeld *et al.* [14] have found experimentally that for phosphated and polymer coated steel a transmission line-type impedance behaviour occurred at the lowest frequencies.

Evaluation of experimental EIS data published so far is often made difficult by the unfortunate tendency to present these data in linear complex plane plots. Since the impedance for coated metals changes over many orders of magnitude between the value for R_Ω at the highest frequencies to that of $R_\Omega + R_{po} + R_p$ at the lowest frequencies, EIS data should be displayed as Bode plots in which the logarithm of the magnitude of the impedance modulus $|Z|$ and the phase angle Φ are plotted against the logarithm of the applied frequency f [25]. Uncritical use of complex plane plots can lead to erroneous conclusions concerning coating degradation. In Fig. 2 theoretical impedance data are presented as Bode plots (Fig. 2(a) and (b)) and complex plane plots (Fig. 2(c)) [26]. Based on Equations 2–4 it has been assumed that coating delamination and corrosion at the coating/metal interface increase from curve 1, which is representative for an intact coating, to curves 2 and 3, which have decreasing values of R_{po} and R_p and increasing values of C_{dl}. While the Bode plots in Fig. 2(a) and (b) clearly indicate coating degradation, the complex plane plots in

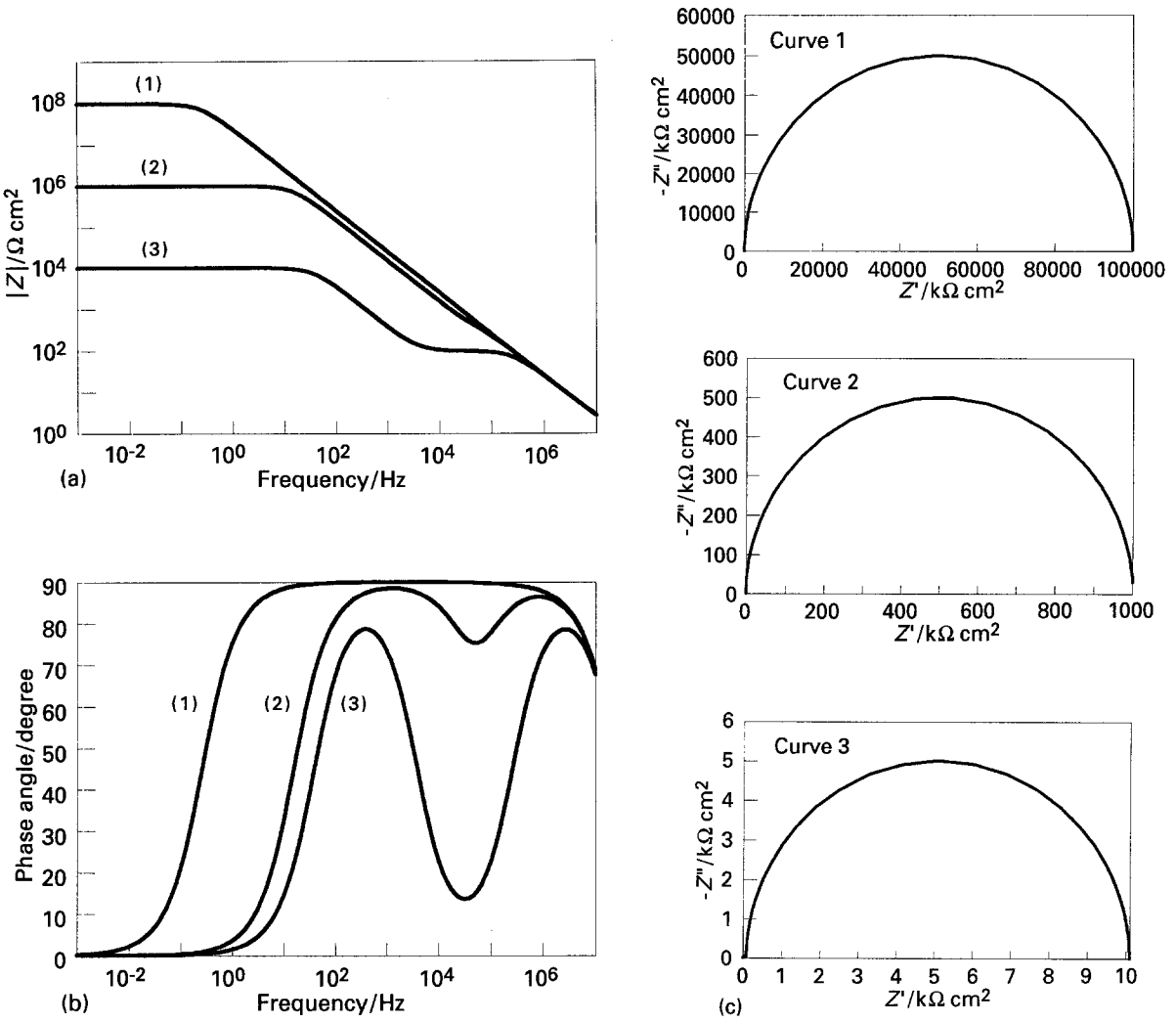

Fig. 2. Theoretical Bode plots ((a) and (b)) and complex plane plots (c) for different degrees of delamination and corrosion rates at the metal/coating interface. $R_\Omega = 1\,\Omega$, $C_c = 6 \times 10^{-9}$ F; curve 1: $R_{po} = 10^4\,\Omega$, $R_p = 10^8\,\Omega$, $C_{dl} = 4 \times 10^{-11}$ F; curve 2: $R_{po} = 10^3\,\Omega$, $R_p = 10^6\,\Omega$, $C_{dl} = 4 \times 10^{-9}$ F; curve 3: $R_{po} = 10^2\,\Omega$, $R_p = 10^4\,\Omega$, $C_{dl} = 4 \times 10^{-7}$ F.

Fig. 2(c) remain unchanged unless the high-frequency data are plotted separately. The phase angle Φ (Fig. 2(b)) is a very sensitive indicator of coating damage. It has to be emphasized at this point that in this review as in the papers of the author on this subject Φ has been assigned positive values, while from an electrical engineering standpoint Φ should be negative. This sign convention is considered to be more convenient in the qualitative analysis of impedance spectra.

Figure 3(a)–(c) shows theoretical impedance spectra which have been calculated for polymer coatings with thicknesses between 10 μm and 1000 μm as a function of the delaminated area fraction $D = A_d/A$ at which corrosion occurs [27]. It was assumed that D increased from $D = 10^{-4}$ to 1.0. The changes of the impedance spectra are due to decreases of R_{po} and R_p and increases of C_{dl} as D increases. With increasing coating thickness the changes of the spectra in the low-frequency region become less pronounced. The changes of parameters such as f_b, f_{min} and Φ_{min} which are defined in Fig. 1(b) and are useful for the analysis of coating damage and corrosion at the metal/coating interface [28, 29] are clearly evident in Fig. 3 as a function of D.

3. Experimental considerations for the collection of EIS data for polymer coated metals and alloys

The very low capacitance and very high resistance values which have to be measured for polymer coated metals require special considerations concerning hardware requirements, procedures for the collection of experimental impedance data and software for the analysis of such data [30–32].

The following considerations concerning hardware and software for collection of experimental EIS data have to be made.

3.1. *Hardware*

Very satisfactory results have been obtained with the Schlumberger model 1250 frequency response analyser (FRA) combined with the Schlumberger model 1286 potentiostat or the Princeton Applied Research potentiostat model 273. The recently introduced Schlumberger model 1255 and 1260 FRAs allow extension of the high-frequency limit of the impedance spectrum to almost 1 MHz, which is important for the recording of the coating capacitance C_c of coatings containing natural or artificial defects (low

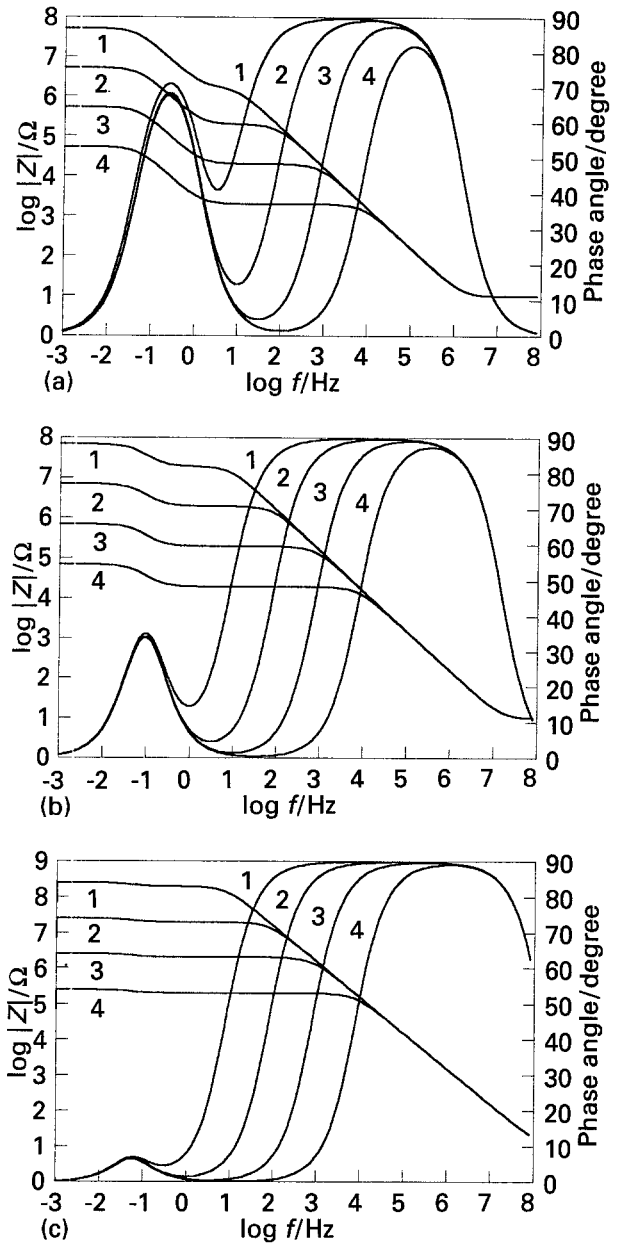

Fig. 3. Simulated impedance spectra for a polymer coated metal as a function of the delamination ratio D; curve 1: $D = 10^{-4}$; curve 2: $D = 10^{-3}$; curve 3: $D = 10^{-2}$; curve 4: $D = 10^{-1}$. $d = 10\,\mu$m (a), $100\,\mu$m (b) and $1000\,\mu$m (c).

values of R_{po} and high values of f_b). Van Westing [33] has compared the performance of these FRAs in the evaluation of coating performance.

3.2. *Software*

Software for the collection of EIS data should allow autoranging of the current measuring resistor and a choice of different data collection procedures in the high and low-frequency region. The software program 'Z-plot' [34] meets these requirements.

3.3. *Experimental requirements*

3.3.1. Electrode size. To lower the experimental values of the resistance and increase the capacitance values the exposed area A of the electrode needs to be increased with increasing coating thickness d [16]. A ratio $A/d > 10^4$ cm provides satisfactory results. Mansfeld and coworkers have been using an area of $20\,cm^2$ for coating thicknesses of $10–50\,\mu$m [14–16, 27–29].

3.3.2. Reference electrode. It is essential to use a pseudo-reference electrode to avoid the phase shift introduced at the highest frequencies when reference electrodes such as the saturated calomel electrode (SCE) are used [35]. This pseudo-reference electrode consists of an SCE capacitively coupled to an inert metal wire such as platinum extending to the tip of the Luggin capillary.

3.3.3. Applied potential. EIS data for polymer coated metals are usually determined at the corrosion potential E_{corr}. Since for very protective coatings a true E_{corr} cannot be measured, a potential close to E_{corr} for the bare metal is often applied. For steel in aerated NaCl a value of -600 mV vs SCE is reasonable.

3.3.4. Frequency range. The frequency range in which data should be collected extends from the highest available frequency to about 1 mHz. This lower limit depends on the coating thickness, exposed area and the extent of coating damage (see Figs 2 and 3). In most cases 5–10 data points equally spaced on a logarithmic scale are measured per decade of frequency.

3.3.5. Current measuring resistor. Since the impedance of polymer coated metals changes over many orders of magnitude, it is extremely important to adjust the current measuring resistor R_m during the course of the measurement [30, 31]. This adjustment ensures that impedance data are measured with equal accuracy at the highest frequencies, where the impedance is low, and the lowest frequencies, where the impedance is very high. In general, R_m should be within a factor of ten of the impedance to be measured. Software such as 'Z-plot' [34] provides autoranging of R_m. It is also possible to record the spectrum in two or more parts with manual adjustment of R_m. The different data sets are then combined in one data file.

3.3.6. A.c. signal. Since a polymer coated metal can be considered a linear system – at least as long as it does not suffer considerable corrosion damage – it is possible to use a larger a.c. signal than for bare metals and thereby to decrease the scatter of the experimental data. A satisfactory approach involves the application of a.c. signals of about 100 mV in the low-frequency range below 1 Hz. Care has to be taken that current overload does not occur.

3.3.7. Data averaging. In order to obtain satisfactory data and reduce the scatter of the experimental data, it is necessary to perform a sufficient number of measurements at each frequency. The use of a

measuring time of 10 s at frequencies exceeding 1 Hz (autointegration off) and collection of data in the frequency range below 1 Hz with the autointegration procedure of Schlumberger model FRAs has provided satisfactory results.

3.3.8. Display of experimental data. It is useful to display the experimental data on the computer screen while they are being measured. In this way, any errors in the set-up of the experiment or problems with the sample can be detected before the entire frequency spectrum has been collected.

3.3.9. Exposure period. In order to determine the corrosion resistance of a polymer coated metal it is often necessary to expose it to a corrosive environment such as 0.5 M NaCl for extended time periods. During this time the impedance spectra will change as the coating properties deteriorate and corrosion occurs at the metal/coating interface. Observed changes of the EIS data can be used for mechanistic interpretation. Sometimes a small defect is applied to the coating which allows analysis of the time dependence and extent of coating delamination and evaluation of the reaction kinetics in the defect [18, 19, 27, 35].

4. Experimental EIS data for polymer coated metals

A literature search concerning applications of EIS to the evaluation of corrosion protection of metals and alloys by polymer coatings has produced a very large number of publications [36–96] which cannot be discussed here in detail. The individual studies include evaluation of water uptake by coatings, degradation of coatings with exposure time, disbonding of coatings, determination of the active area at which corrosion occurs and estimation of corrosion rates at the metal/coating interface. In addition, several papers deal with experimental aspects and/or the interpretation of impedance spectra for polymer coated metals. Mansfeld *et al.* [52, 74] have measured impedance spectra across the coating as well as under the coating using segmented electrodes, while Feser and Stratmann [67] placed a second reference electrode below the polymer film allowing them to measure or control the potential of the metal/polymer coating interface. Simpson *et al.* [65, 75] have developed an atmospheric corrosion monitor (ATMEIS) to follow the degradation of organic coatings during exposure. Skerry *et al.* [57, 59] have combined EIS with potential and current noise measurements and compared the polarization resistance R_p obtained with EIS with the noise resistance R_n obtained from noise measurements. Xiao and Mansfeld [95] have extended this approach by evaluating the frequency dependence of electrochemical noise data and comparing the numerical values and the time dependence of characteristic parameters obtained from EIS and electrochemical noise analysis (ENA). Mansfeld and Tsai [28, 29] have suggested various approaches for evaluating

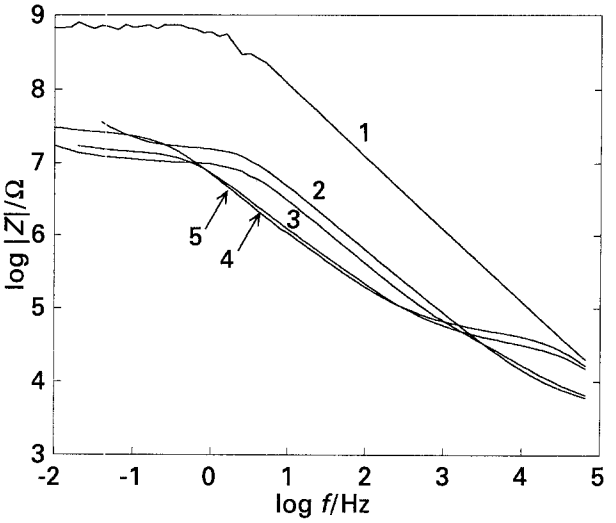

Fig. 4. Bode plots for epoxy coated Al/SiC as a function of exposure to 0.5 M NaCl (open to air). Curves: (1) without a hole, (2–5) with a hole; (2) 3 h; (3) 2 d; (4) 50 d; (5) 90 d.

the remaining lifetime of polymer coatings based on parameters obtained in the high-frequency region of the impedance spectra. Several reviews concerning the application of EIS in the evaluation of the corrosion behaviour of polymer coated metals are available [97–100].

Typical results obtained by the author with EIS for polymer coated metals, alloys and metal-matrix composites (MMC) will be used in the following to illustrate the type of information which can be obtained with the EIS technique. Figure 4 shows experimental EIS data for an epoxy coated ($d = 27\,\mu$m) SiC/Al MMC as a function of exposure time to 0.5 M NaCl [27]. No changes in the impedance spectra were observed over a three months period (curve 1) except for a small increase of C_c corresponding to a water uptake of about 0.8 vol %. In a different experiment with epoxy coated SiC/Al a small hole with a diameter of 0.7 mm was drilled through the coating into the metal in order to study the effects of a coating defect on corrosion at the coating/metal interface and on coating disbonding [27]. Dramatic changes occurred in the impedance spectra which were now totally dominated by the reactions in the defect (curves 2–5 in Fig. 4) except at the highest frequencies where the contribution from C_c can be detected. The pore resistance R_{po} at short exposure times (curves 2 and 3) corresponds to the resistance calculated for the conductivity of NaCl and the dimensions of the hole. With increasing exposure time R_{po} increased presumably due to plugging of the defect with corrosion products observed to cover the hole. The increase of C_{dl} with time is considered to be due to the increased corroding area of the defect (Equation 4).

Impedance spectra for Mg AZ 31 with a Dow 17 pretreatment (thick anodizing) and an Araldite 985 (system A) or Araldite 961 (system B) sealant are shown in Fig. 5 as a function of exposure time to NaCl [27]. The changes of the spectra with increasing exposure time are in agreement with the model in

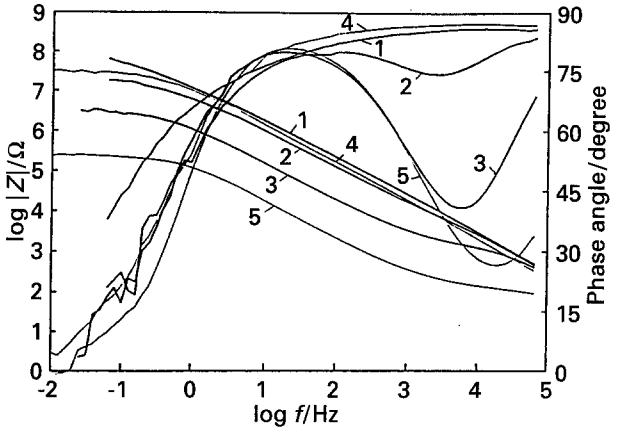

Fig. 5. Bode plots for coated Mg AZ31 as a function of exposure time to 0.5 M NaCl. Curves: (1) 2 d (A); (2) 7 d (A); (3) 14 d (A); (4) 2 h (B); (5) 3 d (B).

Fig. 1(a). For the sample with the Araldite 985 sealant a minimum of the phase angle Φ_{min} was observed at a frequency f_{min} after seven days. After about two weeks the breakpoint frequency f_b, which is the frequency at which the phase angle Φ equals 45°, can also be observed. Figure 6 shows that with increasing exposure time Φ_{min} decreases and f_{min} and f_b move to higher frequencies. These results suggest that parameters such as Φ_{min}, f_{min} and f_b, which are easily measured at relatively high frequencies, are very useful for qualitative monitoring of coating performance. Mansfeld and Tsai [28, 29, 31] have developed this concept further as will be discussed below.

The coating systems in Table 1 applied to cold-rolled steel have been investigated by Mansfeld and Tsai [29] in the as-received condition and after atmospheric exposure at Cape Canaveral, Florida, for two years. Murray and Hack [101] have studied some of the same coatings in the as-received condition. The coating systems CR 1, 2, 5, 6, 8 and 9 were exposed to 0.5 M NaCl in the as-received condition, the coating systems CR 1–7 and 9 were tested after atmospheric exposure. EIS data were obtained at E_{corr} or at −600 mV vs SCE if a stable E_{corr} could not be detected for very protective coatings. The all-latex system CR 8 was so porous that meaningful information concerning coating properties could not be obtained even at very short exposure times.

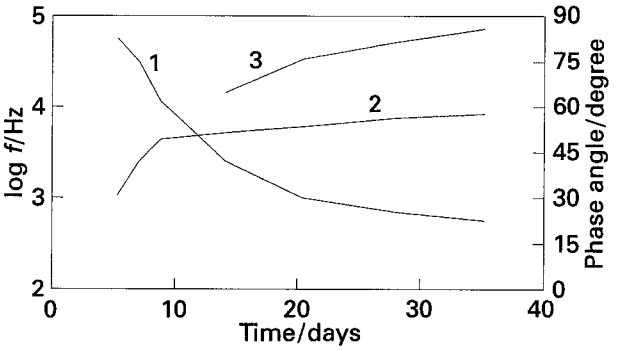

Fig. 6. Time dependence of Φ_{min}, f_{min} and f_b for system A in Fig. 5. Curves: (1) phase angle, Φ_{min}; (2) $\log f_{min}$; (3) $\log f_b$.

Table 1. Coating system components and coating application codes

Code/coat	Primer coat	Second coat	Topcoat
CR1	Alkyd[a]	Enamel alkyd[b]	Enamel alkyd[b]
CR2	Alkyd[a]	Enamel Si-alkyd[c]	Enamel Si-alkyd[c]
CR3	Alkyd[d]	Enamel alkyd[b]	Enamel alkyd[b]
CR4	Alkyd[d]	Enamel Si-alkyd[c]	Enamel Si-alkyd[c]
CR5	Zinc-rich primer[e]	Epoxy polyamide[f]	Polyurethane[g]
CR6	Zinc-rich primer[e]	Epoxy polyamide[f]	Latex[h]
CR7	Epoxy primer[f]	Epoxy polyamide[f]	Latex[h]
CR8	Latex[i]	Latex[h]	Latex[h]
CR9	Epoxy primer[h]	Epoxy polyamide[j]	Epoxy alkyd[k]

[a]TT-P-645. [b]TT-E-489. [c]TT-E-490. [d]SSPC-25. [e]SSPC-20, Type 2. [f]MIL-P-24441 (green). [g]MIL-C-85285. [h]MIL-P-28578. [i]MIL-P-28577. [j]MIL-P-2441 (gray). [k]MIL-P-24441 (white).

Figure 7 shows typical impedance spectra for CR 2 (alkyd primer with enamel silicone alkyd topcoat) after 43, 90 and 162 days exposure to 0.5 M NaCl. For very protective coatings such as CR 6 and 9 the spectra were capacitive and only C_c and R_p could be determined. For CR 1, 2 (Fig. 7) and 5 the impedance spectra changed with exposure time from the capacitive nature typical for intact coatings (Fig. 7, curve (a)) to spectra exhibiting two time constants. After longer exposure times the spectra were dominated by R_{po} (Fig. 7, curves (b) and (c)) at intermediate frequencies. Both f_b and f_{min}, which could be observed after about 90 days for CR 2, shifted to higher frequencies, while Φ_{min} decreased with increasing exposure time.

The results of the fit of the experimental EIS data to the model in Fig. 1(a) are shown in Fig. 8 for CR 1, 2, 5, 6 and 9. The initial coating capacitance C_c was the lowest for CR 9, which apparently has the thickest coating layer (Fig. 8(a)). Coatings CR 1, 2 and 5 seem to have the same thickness. Murray and Hack [101] who investigated an identical set of samples reported average thickness values of 30 μm for CR 1, 104 μm for CR 5 and 6 and 164 μm for CR 9. The increase of C_c in the first days of exposure is considered due to water uptake by the coating. Degradation of the coating during exposure for one year was indicated for CR 1, 2 and 5. Figure 8(b) shows that the pore resistance R_{po} decreased the most for coating

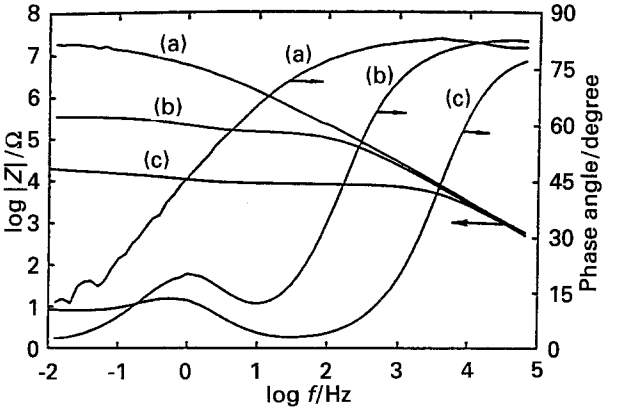

Fig. 7. Impedance spectra for CR 2 after exposure to 0.5 M NaCl for 43 (a), 90 (b) and 162 days (c). $A = 20\,cm^2$.

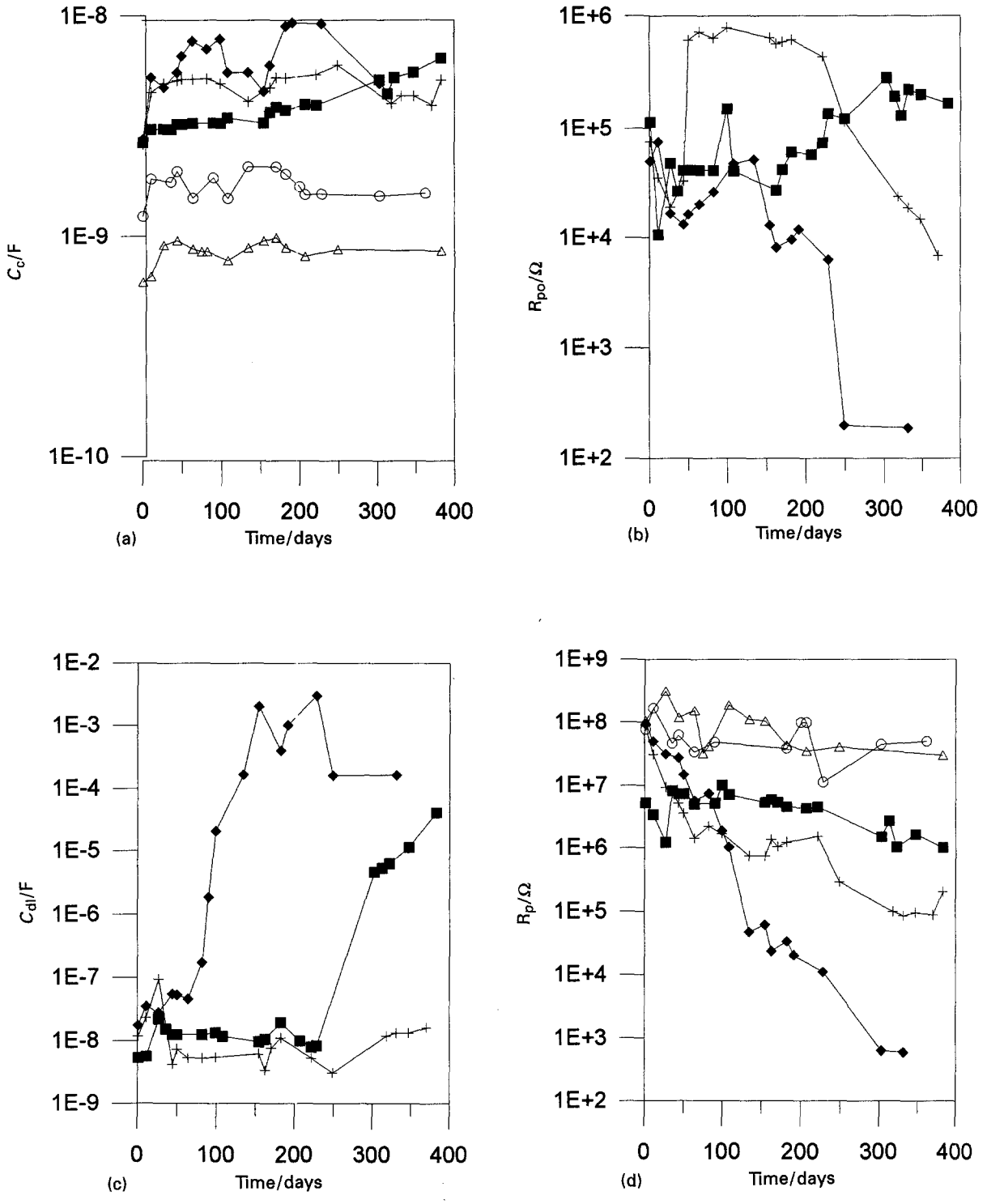

Fig. 8. Time dependence of C_c (a), R_{po} (b), C_{dl} (c), and R_p (d) for CR 1, 2, 5, 6, and 9 exposed to 0.5 M NaCl. Key: (+) CR 1; (◆) CR 2; (■) CR 5; (○) CR 6; (△) CR 9.

CR 2. At the end of exposure, R_{po} was the lowest for CR 2 followed by CR 1 and CR 5. A continuous increase of C_{dl} (Fig. 8(c)) can be considered as evidence that the area at which delamination and/or corrosion occurred was increasing (Equation 4). This increase occurred first and was the largest for CR 2 indicating that this coating system provides the least corrosion protection. It will be noted that for CR 2 C_{dl} reached values as high as several millifarad (Fig. 8(c)). Such a high value cannot be related to the double layer capacitance C_{dl} at the metal/coating interface. A large open blister was observed at the end of the test and it was concluded that the experimental values of C_{dl} and R_p (Fig. 8(d)) are related primarily to this blister. The decrease of R_p, which suggests an increase of the delaminated area at the metal/coating interface (Equation 3), is the largest for CR 2 followed by CR 1 and CR 5 (Fig. 8(d)). This analysis of EIS data for the five coating systems shows qualitatively that coatings CR 1, 2 and 5 suffer degradation and corrosion at the metal/coating interface during exposure to NaCl for one year, while coatings CR 6 and 9 remain more or less unchanged and show excellent performance.

Table 2. Coating parameters and rankings of coating properties for as-received samples

Sample CR	C_c^{0a}	R	dC_c/dt^b	R	dv/dt^c	R	Rust area[d]	R	ΣR	R_T
1	2.66	3	1.90	2	1.23	2	0.92	2	9	2
2	2.80	1	2.49	1	1.46	1	3.81	1	4	1
5	2.70	2	0.41	4	0.32	4	0.02	3	13	3
6	1.24	4	0.60	3	0.90	3	0.00	4	14	4
9	0.62	5	0.036	5	0.13	5	0.00	4	19	5

[a]In 5×10^{-11} F/cm^2 (at $t = 2$ h).
[b]In 5×10^{-12} F/cm^2 day.
[c]In volume %/day.
[d]In % (ASTM D 610 rating, 10 = 0%, 9 = 0.03%, 5 = 3%, 2 = 33%).

As the coating degrades, the real part of the impedance decreases as a result of the formation of conductive paths due to the penetration of corrosive species as well as water uptake. The coating capacitance C_c increases with increasing water uptake. C_c is quite sensitive to water uptake since the dielectric constant of water is about 20 times larger than that of the coating. Bellucci and Niodemo [102] have recently addressed this topic. The volume fraction v of electrolyte absorbed by the coating can be determined from the experimental values of C_c [103, 104]:

$$v = \log \{C_c(t)/C_c(0)\}/\log 80 \qquad (5)$$

where $C_c(t)$ is the coating capacitance at time t and $C_c(0)$ is the initial coating capacitance.

Touhsaent and Leidheiser [104] suggested that the rate of change of the coating capacitance, dC_c/dt, measured at early times can be used to predict the lifetime of polymer coatings. Table 2 summarizes the specific coating capacitance C_c^0 obtained by extrapolation to $t = 0$ (Fig. 8(a) and Equation 1), the rates of changes of the coating capacitance dC_c/dt, the rate of water uptake dv/dt in the first 10 days calculated according to Equation 5, and the percentage of rusted area A_r at 365 days determined according to ASTM D 610 for the coating systems listed in Table 1. It can be seen that dv/dt and dC_c/dt determined at initial times of exposure correlate well with A_r determined after much longer exposure times. An exception is CR 5, for which smaller values of dv/dt and dC_c/dt than for CR 6, but a higher A_r were determined. This result is probably due to the thinner coating for CR 5, which provides less protection. The data in Table 2 can be used to rank the different coating systems in terms of properties which are expected to be related to corrosion protection provided by these coatings. For dv/dt and dC_c/dt CR 2 is ranked first. This coating system also is the thinnest based on the highest value of C_c^0. The same ranking is obtained for visual observation according to which CR 2 has the largest corroded area A_r, while $A_r = 0$ for CR 6 and 9. This result suggests that there is a correlation between water uptake, coating thickness and rusted area. By summing up the individual rankings as $\Sigma R = R_T$, one arrives at the final ranking R_T of the five coatings systems in the order of increasing corrosion protection: $2 < 1 < 5 < 6 < 9$.

Samples which had been exposed to the atmosphere for two years in Florida were also exposed to 0.5 M NaCl. In examining the results of the analysis of the EIS data for these samples a very large initial increase of C_c for CR 2 due to water uptake of the coating is found (Fig. 9(a)). For the same coating without outdoor exposure a much smaller water uptake was observed (Fig. 8(a)). Table 3 provides a summary of the parameters used in Table 2 for the previously exposed samples after exposure to 0.5 M NaCl for 55 days. Comparison of the data in Tables 2 and 3 indicates that previous atmospheric exposure increased the rate of water uptake of these coating systems independent of coating thickness except for CR 1 (alkyd/enamel alkyd), which did not show an increased rate of water uptake. The final ranking

Table 3. Coating parameters and rankings of coating properties for samples after atmospheric exposure for 2Y

Sample CR	C_c^{0a}	R	dC_c/dt^b	R	dv/dt^c	R	Rust area[d]	R	ΣR	R_T
1	3.50	2	1.45	3	0.73	6	< 0.01	5	16	4
2	4.26	1	24.0	1	4.31	1	3.2	1	4	1
3	2.60	3	1.5	2	1.71	2	0.04	2	9	2
4	2.10	4	1.3	4	0.98	4	0.035	3	15	3
5	1.90	5	0.6	6	0.70	7	0.02	4	22	6
6	1.20	6	1.2	5	1.62	3	< 0.01	5	19	5
7	0.97	7	0.37	7	0.75	5	0.00	7	26	7
9	0.55	8	0.034	8	0.67	8	0.00	7	31	8

[a]In 5×10^{-11} F/cm^2 (at $t = 2$ h).
[b]In 5×10^{-12} F/cm^2 day.
[c]In volume %/day.
[d]In % (ASTM D 610 rating, 10 = 0%, 9 = 0.03%, 5 = 3%, 2 = 33%); determined after 55 days.

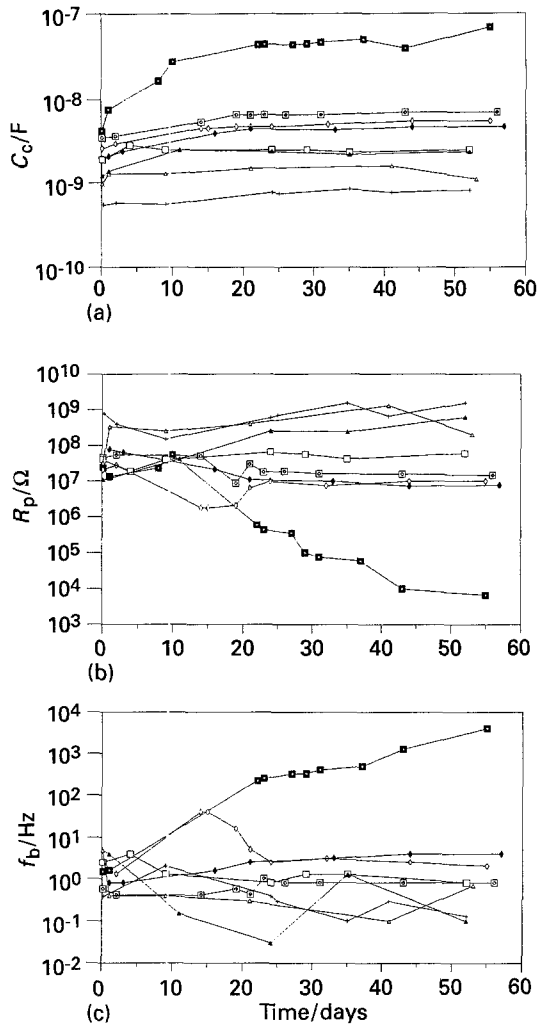

Fig. 9. Time dependence of C_c (a), R_p (b) and f_b (c) during exposure to 0.5 M NaCl for coated steel samples after atmospheric exposure. Key: (□) CR 1; (■) CR 2; (◇) CR 3; (◆) CR 4; (□) CR 5; (▲) CR 6; (△) CR 7; (+) CR 9.

R_T in terms of increasing corrosion protection results in the sequence $2 < 3 < 4 < 1 < 6 < 5 < 7 < 9$. According to the results in Tables 2 and 3 the alkyd systems provide less corrosion protection than coatings with a zinc-rich primer or coatings with an epoxy polyamide primer and an epoxy polyamide or latex topcoat for which excellent performance was observed.

4.1. *Breakpoint frequency method and related approaches*

As discussed above, certain parameters related to coating deterioration can be determined directly from the experimental data without a fit to the model in Fig. 1(a). The breakpoint frequency f_b is related to the delaminated area A_d or the delamination ratio D:

$$f_b = \tfrac{1}{2}\pi R_{po} C_c = (\tfrac{1}{2}\pi R_{po}^{o} C_c^{o})(A_d/A)$$
$$= (2\pi\epsilon\epsilon_o\rho)^{-1} D = f_b^{o} D \qquad (6)$$

with

$$f_b^{o} = (2\pi\epsilon\epsilon_o\rho)^{-1} \qquad (7)$$

Mansfeld and Tsai [28, 29, 31] have suggested that

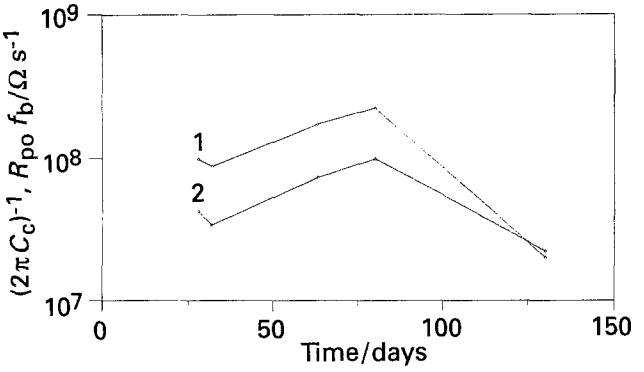

Fig. 10. Time dependence of $\frac{1}{2}\pi C_c$ (curve 1) and $R_{po} f_b$ (curve 2) for CR 2 exposed to 0.5 M NaCl.

in addition to the breakpoint frequency f_b the minimum of the phase angle Φ_{min} and its frequency f_{min} can be used to characterize the extent of coating delamination. Fig. 1(b) is a theoretical Bode plot indicating the location of these parameters. Using the equivalent circuit in Fig. 1(a) and certain simplifying assumptions, it was shown that the following relationships apply:

$$f_{min} = (\tfrac{1}{4}\pi^2 C_c C_{dl} R_{po}^2)^{1/2}$$
$$= (D/4\pi^2\epsilon\epsilon_o C_{dl}^{o}\rho^2 d)^{1/2} = a_1(D)^{1/2} \qquad (8)$$

where $a_1 = (4\pi^2\epsilon\epsilon_o C_{dl}^{o}\rho^2 d)^{-1/2}$

$$\tan\Phi_{min} = (4C_c/C_{dl})^{1/2}$$
$$= (4\epsilon\epsilon_o/C_{dl}^{o} dD)^{1/2} = a_2(D)^{-1/2} \qquad (9)$$

where $a_2 = (4\epsilon\epsilon_o/C_{dl}^{o} d)^{1/2}$

$$f_b/f_{min} = (C_{dl}/C_c)^{1/2} = a_3(D)^{1/2} \qquad (10)$$

where $a_3 = (C_{dl}^{o}/C_c^{o})^{1/2}$.

Mansfeld and Tsai [29] have argued that in using f_b (Equation 6) for the determination of A_d one has to consider that both ϵ and ρ are likely to change with exposure time. Due to water uptake of the coating ϵ will increase, while ρ will decrease as conductive paths and defects develop in the coating. In Equation 7, f_b^{o} is therefore not a constant value, but is likely to change with exposure time as ϵ increases and ρ decreases. In order to decide whether an observed increase of f_b is due to changes in D, ρ or both, Mansfeld and Tsai [29] have proposed the use of Φ_{min} (Equation 9) and the ratio f_b/f_{min} (Equation 10), which are independent of the coating resistivity ρ.

Deflorian *et al.* [105] argued that the product:

$$R_{po} f_b = d/2\pi\epsilon\epsilon_o \qquad (11)$$

should be constant as required by Equations 2 and 6 and suggested that Equation 11 could therefore be used to check the validity of the breakpoint frequency method. However, it has been pointed out [106] that ϵ can change due to water uptake (see Equation 5) which means that $R_{po} f_b = \frac{1}{2}\pi C_c$ is not a constant, but a time dependent experimental parameter (see Fig. 8(a)). It will also be noted that f_b can only be determined for $\Phi_{min} < 45°$. The breakpoint frequency f_{lo} measured for $\Phi_{min} > 45°$ in the low-

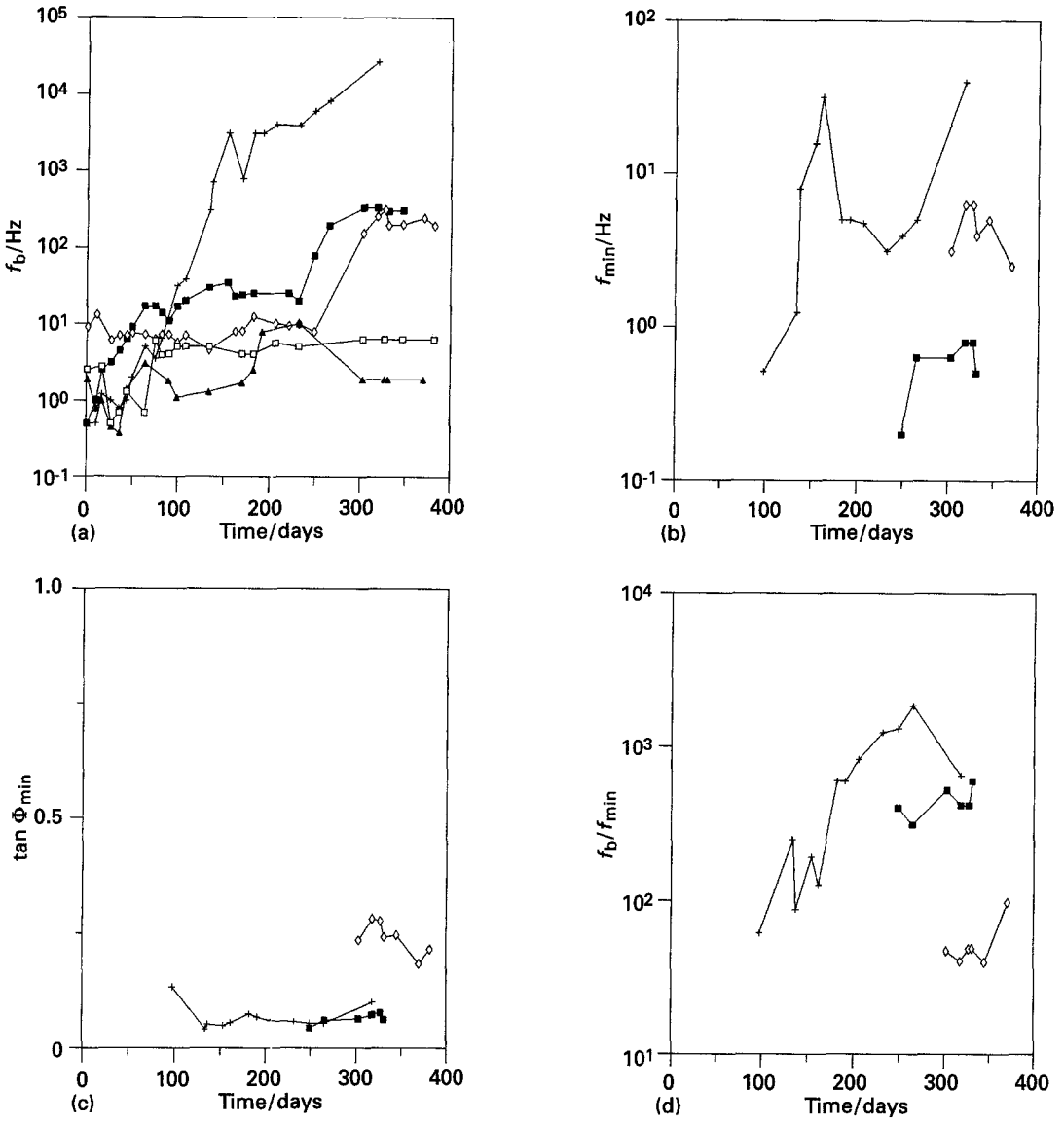

Fig. 11. Time dependence of f_b (a), f_{min} (b), tan Φ_{min} (c) and f_b/f_{min} (d) for coating systems in Table 1. Key: (■) CR 1; (+) CR 2; (◇) CR 5; (◆) CR 6; (□) CR 9.

frequency region (Fig. 1(b)) does not equal f_b as defined in Equation 6, but contains contributions from R_p, R_{po} and C_{dl}. Hack and Scully [108] have discussed the use of f_{lo} in the assessment of coating damage. However, the assumptions on which this approach is based have been criticized [109]. The time dependence of $R_{po}f_b$ reported by Deflorian *et al.* [105], which does not agree with Equation 11, might be due to the use of f_{lo} at early exposure times ($\Phi_{min} > 45°$) and f_b at longer exposure times ($\Phi_{min} < 45°$). Xiao and Mansfeld [110] have obtained good agreement of $R_{po}f_b$ and $\frac{1}{2}\pi C_c$ as required by Equations 2 and 6 for coating system CR 2 exposed to 0.5 M NaCl (Fig. 10). The results in Fig. 10 are close to the theoretical value $R_{po}f_b = \frac{1}{2}\pi C_c^o A = 5.7 \times 10^7\,\Omega\,s^{-1}$ for $t \to 0$ with $C_c^o = 1.4 \times 10^{-10}\,F\,cm^{-2}$ (Table 2) and $A = 20\,cm^2$.

Figure 11 shows the time dependence of f_b, f_{min}, Φ_{min} and f_b/f_{min} for the coating systems in Table 1. The breakpoint frequency f_b (Fig. 11(a)) shows the same time dependence as R_{po} (Fig. 8(b)) with f_b increasing by a factor of about 10^4 for CR 2 and showing smaller increases for CR 1 and 5. Experimental values for f_{min} and Φ_{min} could only be detected for CR 1, 2 and 5 (Fig. 11(b) and (c)). For CR 2 f_{min} increased after about 100 days, for CR 1 f_{min} and Φ_{min} were detected first after 245 days and for CR 5 these parameters could first be recorded after 300 days. These results agree with the finding that CR 2 is the least protective coating followed by CR 1 and CR 5 (Table 2).

An important result concerning the mechanism of coating degradation can be obtained by comparing the numerical values of f_{min} (Fig. 11(b)) and Φ_{min} (Fig. 11(c)). The question is whether changes of these parameters with exposure time are due to changes of D with ρ remaining constant as Haruyama *et al.* [23] have suggested, due to changes of ρ at constant D or due to changes of both parameters. To answer this question it is necessary to expand the analysis given in Equations 6–10, in which only the dependence of the characteristic EIS parameters on coating thickness d, delaminated area A_d and delamination ratio D was considered. As mentioned above, changes due to a decreasing coating resistance, ρ, also have to be taken into account in the analysis of the degradation

of polymer coatings. This consideration leads to the following relationships:

$$R_{po} = \rho d/A_d = \rho d/DA \quad (12)$$

$$f_b = K_b^o D/\rho \quad (13a)$$

$$K_b^o = (2\pi\epsilon\epsilon_o)^{-1} \quad (13b)$$

$$f_{min} = a_4(D)^{1/2}\rho^{-1} \quad (14a)$$

$$a_4 = (2\pi d)^{-1}(C_c^o C_{dl}^o)^{-1/2} \quad (14b)$$

$$\tan\Phi_{min} = a_5(D)^{-1/2} \quad (15a)$$

$$a_5 = 2(C_c^0/C_{dl}^0)^{1/2} \quad (15b)$$

$$f_b/f_{min} = K_b^o(a_4)^{-1}(D)^{1/2} \quad (16a)$$

$$= (C_{dl}^o/C_c^o)^{1/2}(D)^{1/2} \quad (16b)$$

Xiao and Mansfeld [110] have used the ratio $f_b/(f_{min})^2$ which only depends on ρ:

$$f_b/(f_{min})^2 = a_6\rho \quad (17a)$$

$$a_6 = 2\pi d C_{dl}^o \quad (17b)$$

to estimate changes of ρ for coating system CR 2 with exposure time.

Inspection of Equations 12–17 shows that R_{po} and f_b both depend on the ratio ρ/D. On the other hand, f_b/f_{min} and Φ_{min} depend only on D, while $f_b(f_{min})^2$ depends only on ρ. The result that Φ_{min} (Fig. 11(c)) and f_b/f_{min} (Fig. 11(d)) were independent of exposure time for CR 1 and CR 5 after 8 to 10 months suggests that D remained constant during this time. Therefore it can be assumed that the observed decrease of R_{po} (Fig. 8(b)) and the increase of f_b (Fig. 11(a)) for CR 1 and CR 5 are mainly due to a decrease of ρ caused, to some extent, by corrosion products producing mechanical pressure against the polymer layer. The increase of f_b/f_{min} with time at constant Φ_{min} for CR 2 after 160 days seems contradictory to the prediction of Equations 15 and 16. However, examination of CR 2 at the end of the test indicated that a large broken blister (8 mm diam.) filled with corrosion products had formed during that period of time. The direct exposure of the bare steel surface to the corrosive environment is expected to necessitate a change from the model in Fig. 1(a) to a model which includes a contribution from this large, actively corroding area. For a bare metal $f_b' = (2\pi R_\Omega C_{dl})^{-1}$, therefore, f_b' will be larger than f_b for a coated metal if $R_\Omega C_{dl} < R_{po}C_c$ and f_b/f_{min} will also be larger than expected based on Equation 16.

Since the coating thickness is similar for CR 1, 2 and 5, it can be concluded from Fig. 11(c) that D for CR 1 (D_1) is the same as for CR 2 (D_2) and larger than that for CR 5 (D_5): $D_1 = D_2 > D_5$. Based on Equation 17 it follows that $\rho_1 > \rho_2 > \rho_5$. At comparable exposure times, coating system CR 5 (zinc-rich primer with an epoxy polyamide/polyurethane topcoat) had the smallest delaminated area, but a lower coating resistance than CR 1 (alkyd). This discussion shows that it is possible to reach general conclusions concerning coating performance based on experimental

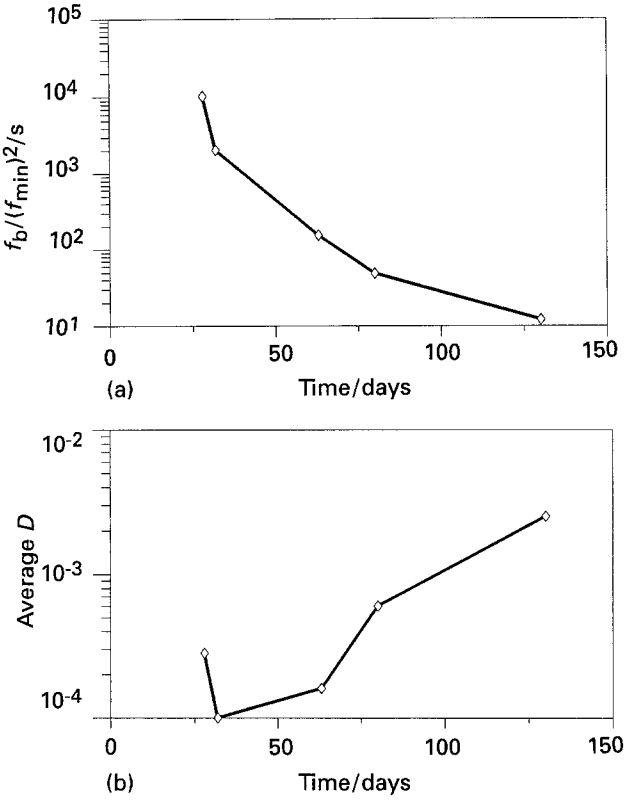

Fig. 12. Time dependence of $f_b/(f_{min})^2$ (a) and D (b) for CR 2 exposed to 0.5 M NaCl.

parameters obtained in the high-frequency region of the impedance spectra.

Xiao and Mansfeld [95] re-examined the performance of CR 2 and CR 9 over a five months time period during which electrochemical noise data were also obtained. The impedance spectra were similar to those reported by Tsai and Mansfeld [29]. Figure 12(a) shows the time dependence of $f_b/(f_{min})^2$ for CR 2. Assuming $d = 25\,\mu m$ and $C_{dl}^o = 30\,\mu F\,cm^{-2}$ (Equation 17) it follows that ρ decreased from $2 \times 10^{10}\,\Omega cm$ after one month to $3 \times 10^7\,\Omega cm$ after five months [110]. The same authors have also estimated the changes of D with time for the same coating system. The results in Fig. 12(b) were calculated assuming $D = 10^{-4}$ after 32 days as an average value from the time dependence of R_p (Equation 3), C_{dl} (Equation 4), Φ_{min} (Equation 9) and f_b/f_{min} (Equation 10). An increase of D by about a factor of 10 to 20 was obtained from the last three parameters, while a much larger increase of D was calculated from R_p. Apparently R_p^o in Equation 3 was not constant, but changed as the coating disbonded and corrosion became more pronounced.

For the previously exposed samples, a decrease of R_p (Fig. 9(b)) and an increase of f_b (Fig. 9(c)) were only observed for CR 2 in the exposure time of 55 days. Comparison of the changes of f_b, f_{min}, $\tan\Phi_{min}$ and f_b/f_{min} for CR 2 in Fig. 13, in which the data for the as-received and previously exposed samples are compared, suggests that the mechanisms of coating degradation and initiation of corrosion are similar, but that these processes occur at a faster rate for the previously exposed sample. The continuous decrease of Φ_{min} with time indicates that rapid

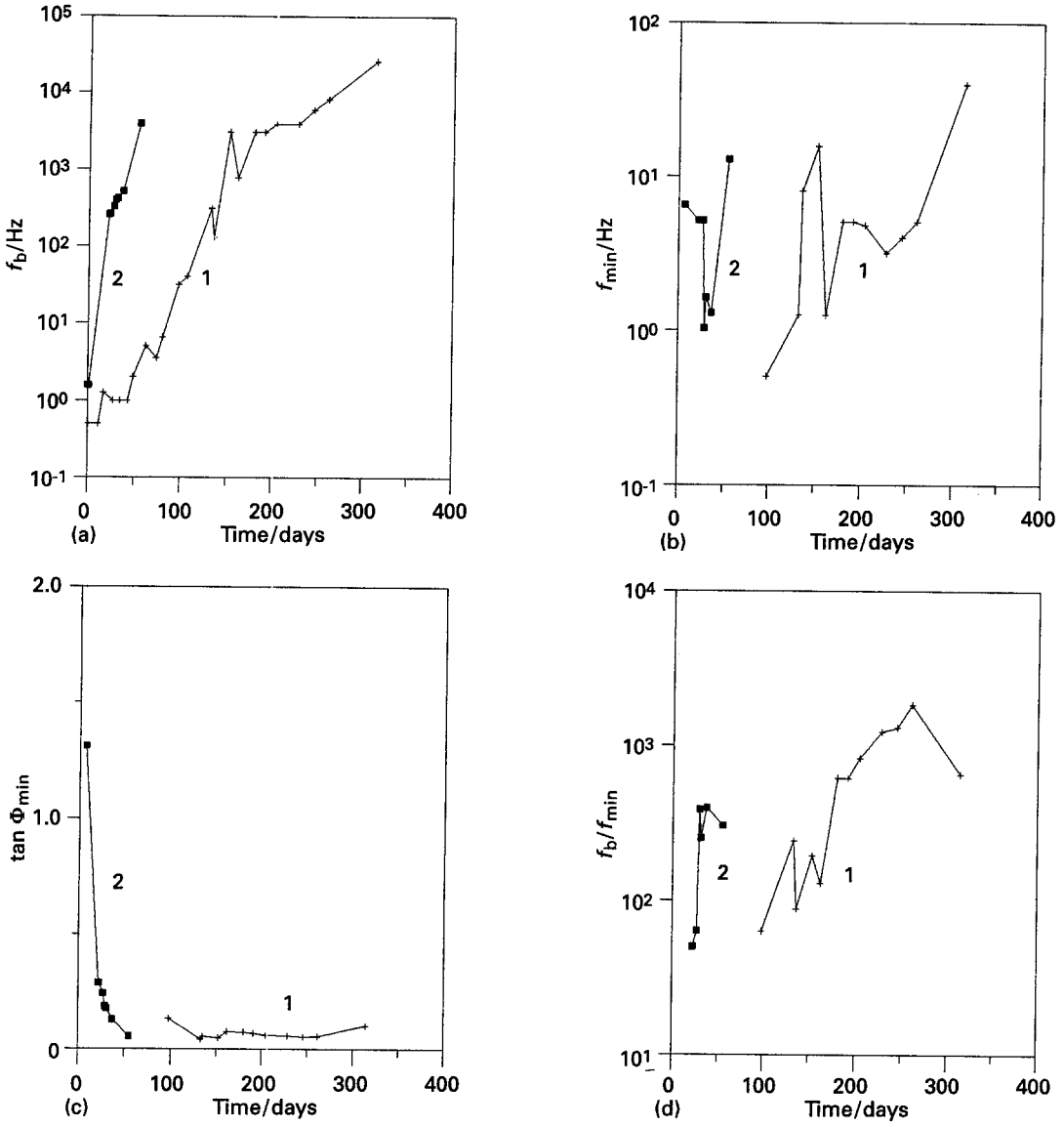

Fig. 13. Time dependence of f_b, f_{min}, tan Φ_{min} and f_b/f_{min} for CR 2, as-received (curve 1) and after atmospheric exposure (curve 2), during exposure to 0.5 M NaCl.

delamination occurred for CR 2 already during the first few weeks of exposure to 0.5 M NaCl as a result of previous atmospheric exposure. High values of R_p ($>10^7\,\Omega$) (Fig. 9(b)) and low values of $f_b < 10$ Hz (Fig. 9(c)) for the other coating systems suggest that these systems were still protective during this short test period in 0.5 M NaCl despite previous atmospheric exposure.

For field studies, in which qualitative evaluation of coating damage in a short time is of interest, measurement of the impedance at two frequencies has been proposed [29, 31]. If these frequencies are located in the capacitive region, where the slope of the $\log|Z| - \log f$ plot has a theoretical value of -1, then the ratio of the two measured impedance data is the same as the ratio of the frequencies. With increasing coating damage, this ratio R decreases due to the decrease of R_{po}. In Fig. 14 the ratios R_1 and R_2 are plotted as a function of D, where R_1 and R_2 are defined as

$$R_1 = \log(Z_{100}/Z_{10000}) \quad (18)$$

$$R_2 = \log(Z_1/Z_{100}) \quad (19)$$

with Z_1 being the impedance at the frequency f_1 and $0 \leq R_1 \leq 2$ (Fig. 14). For a perfect coating for which the impedance is capacitive in the entire measured frequency region $R_1 = R_2 = 2$. If a contribution

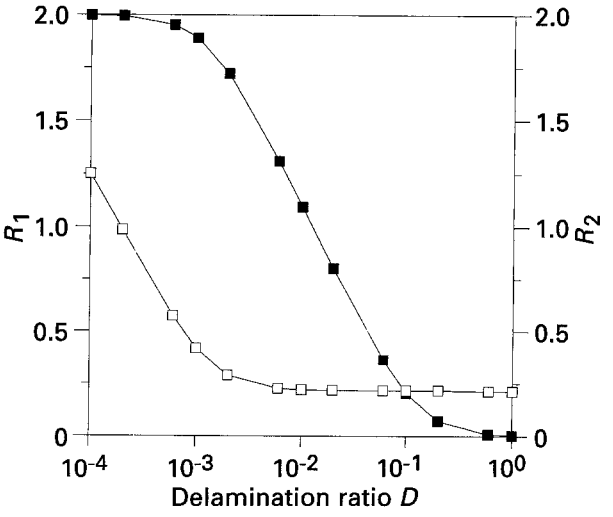

Fig. 14. Theoretical plots of R_1 (■) and R_2 (□) as a function of D for $d = 10\,\mu$m.

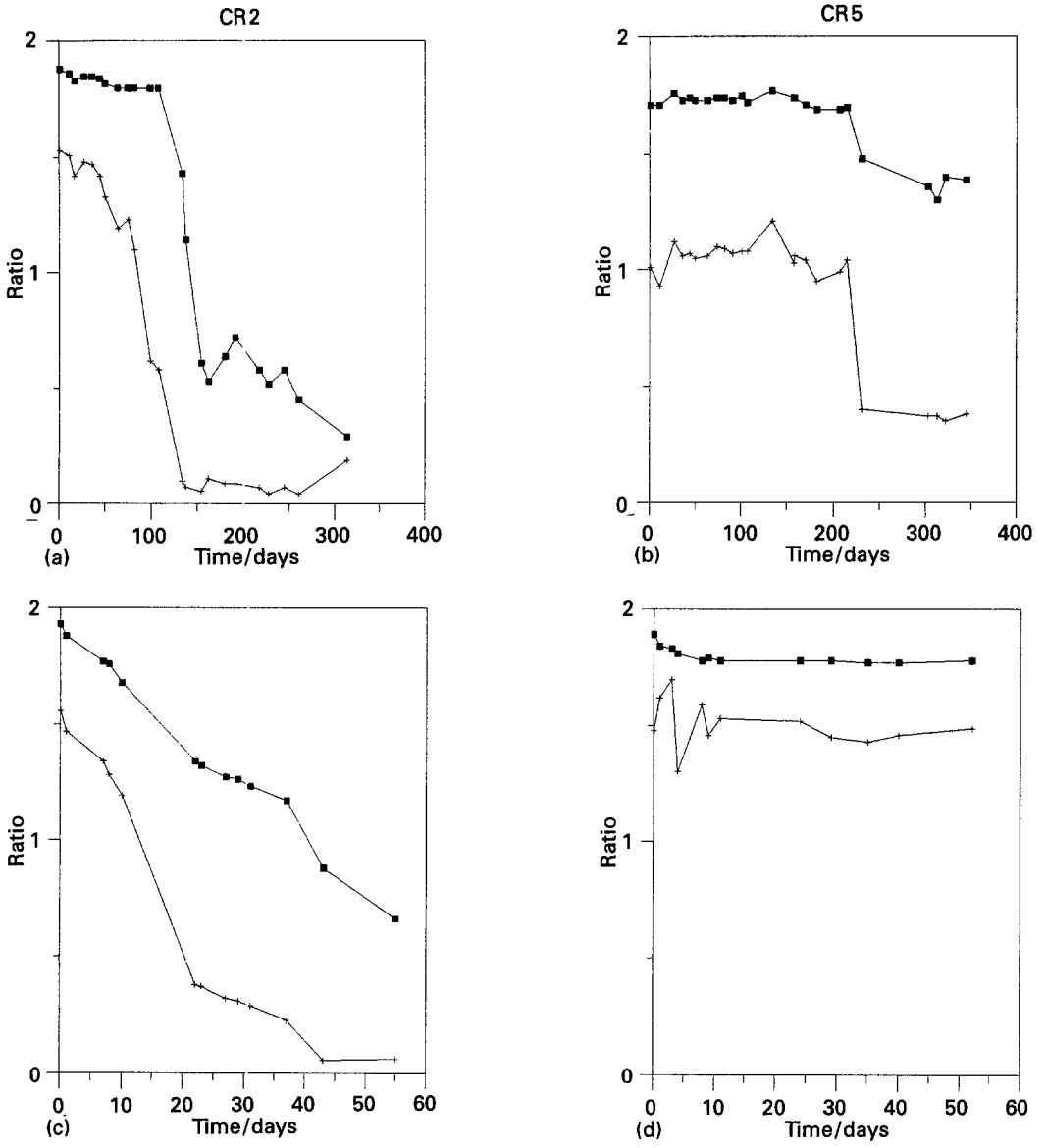

Fig. 15. Time dependence of R_1 (■) and R_2 (□) during exposure to 0.5 M NaCl for as-received CR 2 (a) and CR 5 (b) and for previously exposed CR 2 (c) and CR 5 (d).

from R_{po} appears in the frequency range in which R_1 or R_2 are determined, R_1 and/or R_2 will decrease with decreasing R_{po}. R_1, which is determined at the higher frequencies, is independent of the coating thickness d and is most sensitive to coating damage for values of D between 10^{-3} and 0.1 [31]. R_2 depends slightly on d for thin coatings. It is most useful for $D < 10^{-3}$ and is therefore more applicable in the very early stages of coating degradation [31]. Figure 14 is plotted for $d = 10\,\mu m$.

The time dependence of R_1 and R_2 for as-received samples confirmed that coating degradation was the largest for CR 2 followed by CR 1 and CR 5. A comparison of experimental data for CR 2 and CR 5 (as-received against pre-exposed) is given in Fig. 15. For as-received CR 2 and 5, R_2 was between 1.0 and 1.5 at the beginning of the test (Fig. 15(a) and (b)) which according to the theoretical plots in Fig. 14 suggests that the initial values of D were about 10^{-4}. For CR 6 and 9, D apparently did not exceed 10^{-4} over the entire one-year test period. For the previously exposed CR 2, the continuous decrease of R_1 and R_2 confirms that rapid coating degradation occurred during exposure to 0.5 M NaCl (Fig. 15(c)). For CR 1, 3, 4 and 5 D was about 10^{-4} at the beginning of the test, but did not change much over the next 55 days as shown in Fig. 15(d) for CR 5. For CR 6, 7 and 9 R_1 and R_2 had values close to 2 over the entire test period indicative of excellent coating performance despite previous atmospheric exposure.

The advantage of the breakpoint frequency method in its original and extended form lies in the possibility to detect coating damage and loss of corrosion protection in a short time. The values of f_b and f_{min} typically are located at frequencies higher than 1 Hz. If a frequency scan is carried out starting at the highest frequencies and ending when f_b and/or f_{min} have been detected, the measurement can be carried out in a few minutes. This approach allows qualitative evaluation of a large number of samples or different areas on a large sample in a reasonable time period and is therefore especially useful for corrosion monitoring.

The same considerations apply for the use of R_1 and R_2.

The breakpoint frequency method has attracted the attention of many authors. Although the usefulness of this method has been recognized generally, it does not seem entirely clear what quantity is measured with this method, that is, whether the area of pores and defects in the coating is determined or the wetted area at which the coating is delaminated and active corrosion occurs. It will be noted that the wetted area usually contains an anodic part which is surrounded by the cathode. Originally, Haruyama *et al.* [23] suggested that f_b is related to A_d since the current flow during the impedance measurement is concentrated at areas where the coating has delaminated. Kendig [107] in a discussion of a paper by Mansfeld and Tsai [28] disagreed with this view citing results obtained by Kendig *et al.* [15] for a free film of polybutadiene. A more detailed discussion of this subject has been presented by Kendig *et al.* [22]. Mansfeld and Tsai [28, 29] have pointed out that R_{po} (Equation 2) and f_b (Equation 13) depend both on ρ and A_d. Hack and Scully [108] citing data obtained by Scully [111] suggested that very fine pores penetrated the polymer coating and that f_b was related therefore to the area of these pores. This explanation has been criticized [109] since it is unlikely that these fine pores penetrate coatings with $d = 100\,\mu m$ already at the earliest exposure times. In addition, many coatings develop blisters which is not possible in the presence of such pores. Deflorian *et al.* [105] concluded that the breakpoint frequency method does not apply in the early stages of degradation ($D < 5 \times 10^{-4}$) and that f_b corresponds to the area of pores and defects in the coating. These arguments were based on Equation 11 and experimental data obtained by the authors. However, as already discussed above in relation to Equation 11, this view cannot be supported by these authors' experimental data and analysis [106]. Since f_b can only be measured for $\Phi_{min} < 45°$, it follows from Equation 9 that for most coatings the lower limit for D is about 10^{-4}. This corresponds to a circular area with a radius of about $200\,\mu m$ for an exposed area of $20\,cm^2$. Even smaller values of D can be determined based on f_{min} and Φ_{min}. EIS is therefore a very suitable technique for detection of degradation of polymer coatings and initiation of corrosion at the metal/coating interface at the very early stages. For mechanistic studies analysis of the EIS data and correlation of the parameters in the EC of Fig. 1(a) – or other ECs for more complicated coatings systems such as coated, phosphated metals – with coating properties can be carried out. It will be noted that the area at which corrosion occurs, which has been assumed in this review to be similar to A_d, needs to be known for calculation of corrosion rates at the metal/coating interface. For purposes of corrosion monitoring, the breakpoint frequency methods and the other approaches discussed above have been shown to provide meaningful results.

5. Summary and conclusions

The availability of software for the collection of EIS data for polymer coated metals and alloys has made it relatively easy to obtain high-quality impedance data for these systems. This review has shown that most impedance spectra reported in the literature can be fitted to the simple model in Fig. 1(a) or to slightly more complicated equivalent circuits. Software based on these models is available for the analysis of experimental impedance data. For very protective coatings the spectra are capacitive. From the coating capacitance C_c the water uptake of the coating can be determined as a function of exposure time according to Equation 5 or more sophisticated models [102]. As damage to the coating occurs resulting in a decreased coating resistivity ρ, the pore resistance R_{po} decreases. Eventually disbonding of the coating is observed by the changes of the polarization resistance R_p and the capacitance C_{dl} which both are related to the delaminated area A_d or the delamination ratio D. A qualitative evaluation of changes of A_d or D with time can be obtained by observing changes of R_p and C_{dl}. A quantitative determination of these parameters is difficult since the numerical values of R_p^o and C_{dl}^o are usually not known and might not be constant during the entire exposure time. Since R_{po} depends on the ratio ρ/D, it is not possible to determine the changes of these two parameters with exposure time based on R_{po} alone.

A fit of experimental impedance data to the model in Fig. 1(a) or other appropriate models allows a complete analysis of the properties of the polymer coating and the metal/coating interface and their changes with exposure time. Using certain assumptions it is often possible to obtain information concerning the initiation and propagation of damage to the coating as well as corrosion at the metal/coating interface. However, for corrosion monitoring in field applications or for screening of a large number of samples the relatively long time period necessary for collecting the entire impedance spectrum might present a problem. In these situations the breakpoint frequency method and its extension discussed in this review present an attractive alternative. The breakpoint frequency f_b (Equation 13) and other parameters such as f_{min} (Equation 14) and Φ_{min} (Equation 15) as well as certain combinations of these parameters (Equations 16 and 17) can be determined at relatively high frequencies ($f > 1$ Hz) in a short time. It has to be remembered that several breakpoint frequencies exist in an impedance spectrum for a coating system with reduced protective properties (Fig. 1(b)). In the analysis of such spectra it has to be considered that f_b is defined only for $\Phi_{min} < 45°$. The correlations of f_b, f_{min}, Φ_{min}, f_b/f_{min} and $f_b/(f_{min})^2$ with ρ and D have been presented in this review. By applying these correlations to experimental impedance spectra for a number of different coating systems on cold rolled steel exposed to NaCl, it has been possible to demonstrate for systems with relatively poor performance at

what time and to what extent coating damage (decrease of ρ) and disbonding (increase of A_d or D) occur. Therefore, it has been shown that a complete analysis of the performance of a coating system is possible based on EIS data collected at relatively high frequencies.

For corrosion monitoring applications a two-frequency method has been proposed (Equations 18 and 19, Fig. 14). Since it is possible to obtain many measurements in a very short time with this method and since EIS is a nondestructive technique, it can be used to screen a large number of test panels repeatedly. It is also possible to evaluate the properties of a paint system on different areas of a large structure and to use this information to decide where the paint has to be replaced. It is suggested that the two-frequency method can form the basis of an instrument for field testing of protective polymer coatings.

References

[1] G. Menges and W. Schneider, *Kunststofftechnik* **12** (1973) 265, 316 and 343.
[2] H. Potente and E. Braches, *Adhesion* **11** (1979) 34.
[3] J. D. Scantlebury and K. N. Ho, *J. Oil Colour Chem. Assoc.* **62** (1979) 89.
[4] L. Beaunier, I. Epelboin, J. C. Lestrade and H. Takenouti, *Surface Techn.* **4** (1976) 237.
[5] G. Reinhard, D. Scheller and K. Hahn, *Plaste Kautsch.* **22** (1975) 56.
[6] G. Reinhard and K. Hahn, *ibid.* **22** (1975) 361.
[7] G. Reinhard, K. Hahn and R. Kaltofen, *ibid.* **22** (1975) 522.
[8] G. Reinhard, K. Hahn and B. Gorzolla, *ibid.* **25** (1978) 548.
[9] G. Reinhard and K. Hahn, *ibid.* **26** (1979) 580.
[10] G. Reinhard, K. Hahn and H. M. Wittich, *ibid.* **27** (1980) 709.
[11] G. Reinhard, K. Hahn and U. Rammelt, *ibid.* **28** (1981) 51.
[12] F. Mansfeld, H. Shih, H. Greene and C. H. Tsai, *ASTM STP* **1188** (1993) 37.
[13] B. Boukamp, *Solid State Ionics* **20** (1986) 31.
[14] F. Mansfeld, M. Kendig and S. Tsai, *Corrosion* **38** (1982) 478.
[15] M. Kendig, F. Mansfeld and S. Tsai, *Corr. Sci.* **23** (1983) 317.
[16] F. Mansfeld and M. Kendig, *ASTM STP* **866** (1985) 122.
[17] M. Kendig and J. Scully, *Corrosion* **46** (1990) 22.
[18] J. Titz, G. H. Wagner, H. Spaehn, M. Ebert, K. Juettner and W. J. Lorenz, *in* 'Advances in Corrosion Protection by Organic Coatings', *Electrochem. Soc., Proc.* **89-13** (1989) 261.
[19] J. Titz, G. H. Wagner, H. Spaehn, M. Ebert, K. Juettner and W. J. Lorenz, *Corrosion* **46** (1990) 221.
[20] R. D. Armstrong and J. D. Wright, *Corr. Sci.* **33** (1992) 1529.
[21] R. D. Armstrong, J. D. Wright and T. M. Handyside, *J. Appl. Electrochem.* **22** (1992) 795.
[22] M. W. Kendig, S. Jeanjaquet and J. Lumsden, *ASTM STP* **1188** (1993) 407.
[23] S. Haruyama, M. Asari and T. Tsuru, *in* 'Corrosion Protection by Organic Coatings', *Electrochem. Soc., Proc.* **87-2** (1987) 197.
[24] R. Hirayama and S. Haruyama, *Corrosion* **47** (1991) 952.
[25] F. Mansfeld, *Corrosion* **44** (1988) 558.
[26] F. Mansfeld and M. W. Kendig, Proc. Int. Cong. Metall. Corr., 3-74, June 1984, Toronto, Canada.
[27] F. Mansfeld, C. H. Tsai and H. Shih, *in* 'Advances in Corrosion Protection by Organic Coatings', *Electrochem. Soc., Proc.* **89-13** (1989) 228.
[28] F. Mansfeld and C. H. Tsai, *Corrosion* **47** (1991) 958.
[29] C. H. Tsai and F. Mansfeld, *ibid.* **49** (1993) 726.
[30] M. Kendig, A. Allen and F. Mansfeld, *J. Electrochem. Soc.* **131** (1984) 935.
[31] C. H. Tsai, Ph.D. thesis, University of Southern California, Aug. 1992.
[32] Schlumberger Application, note no. 26.
[33] E. van Westing, 'Determination of Coating Performance with Impedance Measurements', TNO Center for Coatings Research, Delft, The Netherlands, 1992.
[34] Z-plot, Scribner Assoc., Charlottesville, VA, USA.
[35] F. Mansfeld, S. Lin, V. C. Chen and H. Shih, *J. Electrochem. Soc.* **135** (1986) 906.
[36] F. M. Geenen, J. H. W. DeWit and E. P. M. Van Westing, *Prog. Org. Coat.* **18** (1990) 299.
[37] S. Spindler, *Plaste Kautsch.* **29** (1982) 542.
[38] G. Reinhard and K. Hahn, *ibid.* **30** (1983) 292.
[39] M. Kendig, S. Tsai and M. Mansfeld, *Mater. Perform.* **23**(6) (1984) 37.
[40] J. Hubrecht, J. Vereecken and M. Piens, *J. Electrochem. Soc.* **131** (1984) 2010.
[41] G. Reinhard and U. Rammelt, *Korrosion* **15** (1984) 175.
[42] U. Rammelt and G. Reinhard, *J. Electroanal. Chem. Interfacial Electrochem.* **180** (1984) 327.
[43] J. Hubrecht and J. Vereecken, Proc. Int. Cong. Metall. Corros. 3-85, Toronto, Canada, June 1984.
[44] M. Morcillo, J. Simancas, J. Bastidas, S. Feliu, C. Blanco and F. Camon, *Polym. Mater. Sci. Eng.* **53** (1985) 378.
[45] F. Mansfeld and M. W. Kendig, *Werkst. Korros.* **36** (1985) 473.
[46] J. F. McIntyre and H. Leidheiser, Jr., *J. Electrochem. Soc.* **133** (1986) 43.
[47] G. Reinhard, U. Rammelt and K. Rammelt, *Corr. Sci.* **26** (1986) 109.
[48] F. Mansfeld and M. Kendig, *Org. Coat.* **8** (1986) 513.
[49] F. Mansfeld and M. Kendig, *Mater. Sci. Forum* **8** (1986) 337.
[50] P. Giminez, D. Petit and M. Badia, *ibid.* **8** (1986) 315.
[51] T. Picaud, M. Duprat and F. Dabosi, *ibid.* **8** (1986) 303.
[52] F. Mansfeld and S. Jeanjaquet, *Corr. Sci.* **26** (1986) 727.
[53] F. Mansfeld, S. Jeanjaquet and M. W. Kendig, *ibid.* **26** (1986) 735.
[54] J. P. Lomas, L. M. Callow and J. D. Scantlebury, *ACS Symp. Ser.* **322** (1986) 31.
[55] F. Mansfeld, S. Jeanjaquet and M. W. Kendig, Proc. Symp. Corros. Prot. Org. Coat., *Electrochem. Soc., Proc.* **87-2** (1987) 217.
[56] H. Leidheiser, Jr., R. D. Granata and R. Turoscy, *Corrosion* **43** (1987) 296.
[57] B. S. Skerry and D. A. Eden, *Prog. Org. Coat.* **15** (1987) 269.
[58] C. Compere, J. J. Hechler, K. C. Cole, C. P. Vijayan and C. M. Davidson, *Polym. Mater. Sci. Eng.* **58** (1988) 315.
[59] B. S. Skerry, A. Alavi and K. I. Lindgren, *J. Coat. Techn.* **60** (1988) 97.
[60] B. Fastrup and A. Saarnak, *Prog. Org. Coat.* **16** (1988) 277.
[61] J. Hubrecht and J. Vereecken, Proc. Symp. Transient Techn. Corros. Sci. Eng., *Electrochem. Soc., Proc.* **89-1** (1989) 266.
[62] I. Sekine, K. Moriya and M. Yuasa, *Boshoku Gijutsu* **38** (1989) 365.
[63] S. Feliu, J. C. Galvan and M. Morcillo, *Prog. Org. Coat.* **17** (1989) 143.
[64] K. Umeyama, S. Takai and T. Tsuru, Proc. Symp. Adv. Corros. Prot. Org. Coat., *Electrochem. Soc., Proc.* **89-13** (1989) 241.
[65] T. Simpson, P. J. Moran, H. Hampel, G. D. Davis, B. A. Shaw, C. Arah, T. L. Fritz and K. Zankel, *Corrosion* **46** (1990) 331.
[66] D. M. Drazic and V. B. Miskovic-Stankovic, *Corr. Sci.* **30** (1990) 575.
[67] R. Feser and M. Stratmann, *Steel Res.* **61** (1990) 482.
[68] A. Miszczyk and J. Bordzilowski, *Farbe Lack* **96** (1990) 860.
[69] D. M. Drazic and V. B. Miskovic-Stankovic, *Prog. Org. Coat.* **18** (1990) 253.
[70] G. Shaw, C. E. Rogers and J. H. Payer, *J. Coat. Techn.* **63** (1991) 35.
[71] G. W. Walter, *Corr. Sci.* **32** (1991) 1059.
[72] *Idem, ibid.* **32** (1991) 1085.
[73] C. T. Chen and B. S. Skerry, *Corrosion* **47** (1991) 598.
[74] F. Mansfeld, S. L. Jeanjaquet and M. W. Kendig, Proc. Adv. Localized Corrosion, NACE-9 (1990) 343.
[75] T. Simpson, P. J. Moran, H. Hampel, G. D. Davis, B. A. Shaw, C. O. Arah, T. L. Fritz and K. L. Zankel, *ASTM STP* **1000** (1990) 397.
[76] F. M. Geenen and J. H. W. DeWit, *Farbe Lack* **98** (1992) 9.
[77] K. Micka and L. Kavan, *Electrochim. Acta* **37** (1992) 997.
[78] U. Rammelt and G. Reinhard, *Farbe Lack* **98** (1992) 261.

[79] M. D. Maksimovic and V. B. Miskovic-Stankovic, *Corr. Sci.* **33** (1992) 271.
[80] I. Nowosz-Arkuszewa and M. Krawczyk, *ibid.* **33** (1992) 861.
[81] E. Frechette, C. Compere and E. Ghali, *ibid.* **33** (1992) 1067.
[82] F. Bellucci, L. Nicodemo, T. Monetta, M. J. Kloppers and R. M. Latanision, *ibid.* **33** (1992) 1203.
[83] S. A. McCluney, S. N. Popov, B. N. Popov, R. E. White and R. B. Griffin, *J. Electrochem. Soc.* **139** (1992) 1556.
[84] F. Mansfeld, Discussion of [76], *J. Electrochem. Soc.* **140** (1993) 1825.
[85] W. S. Tait, K. A. Handrich, S. W. Tait and J. Martin, *ASTM STP* **1188** (1993) 428.
[86] S. Feliu Jr., R. Barajas, J. M. Bastidas, M. Morcillo and S. Feliu, *ibid.* **1188** (1993) 438.
[87] R. D. Granata and K. J. Kovaleski, *ibid.* **1188** (1993) 450.
[88] R. Armas, C. A. Gervasi, A. DiSarli, S. G. Real and J. R. Vilche, *Corrosion* **48** (1992) 379.
[89] I. Sekine, K. Sakaguchi and M. Yuasa, *J. Coat. Techn.* **64** (1992) 45.
[90] C. Compere, J. J. Hechler and K. Cole, *Prog. Org. Coat.* **20** (1992) 187.
[91] A. Amirudin, C. Barreau and D. Thierry, *Mater. Sci. Forum* **111–112** (1992) 291.
[92] A. H. Al-Hashem and K. J. Habib, *J. Coat. Techn.* **64** (1993) 101.
[93] B. N. Popov, M. A. Alwohaibi and R. E. White, *J. Electrochem. Soc.* **140** (1993) 947.
[94] M. J. L. Oestergaard, A. Visgaard and E. Maahn, *Surf. Coat. Int.* **76** (1993) 29.
[95] H. Xiao and F. Mansfeld, *J. Electrochem. Soc.* **141** (1994) 2332.
[96] F. Mansfeld and M. W. Kendig, Proc. Int. Cong. Met. Corros. 3-74, Toronto, Canada, June 1984.
[97] K. Juettner, W. J. Lorenz, W. Paatsch, M. W. Kendig and F. Mansfeld, *Werkst. Korros.* **36** (1985) 120.
[98] F. Mansfeld, *Corrosion* **44** (1988) 856.
[99] *Idem, Electrochim. Acta* **35** (1990) 1533.
[100] *Idem, NATO ASI Ser., Ser. E* **203** (1991) 521.
[101] J. Murray and H. Hack, *Corrosion* **48** (1992) 671.
[102] F. Bellucci and L. Niodemo, *ibid.* **49** (1993) 235.
[103] D. M. Brasher and A. H. Kingsbury, *J. Appl. Chem.* **4** (1954) 62.
[104] R. Touhsaent and H. Leidheiser, Jr., *Corrosion* **28** (1972) 435.
[105] F. Deflorian, L. Ferizzi and P. L. Bonora, *Electrochim. Acta* **38** (1993) 1609.
[106] F. Mansfeld, discussion of [105], submitted to *Electrochim. Acta.*
[107] M. W. Kendig, *Corrosion* **47** (1991) 964.
[108] H. P. Hack and J. R. Scully, *J. Electrochem. Soc.* **138** (1991) 33.
[109] F. Mansfeld, discussion of [101], *ibid.* **139** (1992) 639.
[110] H. Xiao and F. Mansfeld, unpublished results.
[111] J. R. Scully, *J. Electrochem. Soc.* **136** (1989) 979.